Electronic Supplementary Material (ESI) for Physical Chemistry Chemical Physics.

Supporting information for

An electrochemical study on $LiMn_2O_4$ for Al^{3+} ion storage in aqueous electrolytes

Sunny Nandi[a], Shyamal K. Das[#a]

[a]Department of Physics,Tezpur University, Assam 784028, India

Experimental details:

Commercially available $LiMn_2O_4$ was used for this study. It was purchased from Sigma Aldrich (Product No. 482277) and no further treatment was performed prior to the study. The electrode slurry was prepared by mixing $LiMn_2O_4$ powder with carbon black (Alfa Aesar Product No. H30253) and polyvinylidene fluoride (PVDF) (Sigma Aldrich, Product No. 182702) with weight proportion of 70:20:10 in N-methyl-2-pyrrolidone (NMP). This prepared slurry was coated on titanium (Ti) substrate (breadth 1 cm and length 1.5 cm) and dried at 120 ^{o}C for 12 hr. The coated area is 1 cm^2. The mass loading of the material was approximately 2.5-3.5 mg.

The cyclic voltammetry (CV) and galvanostatic charge/discharge experiments were performed in a cylindrical glass cell (diameter 2.7cm, height 2.2 cm) using Biologic SP300 electrochemical work station. Pt electrode and aqueous Ag/AgCl electrode were used as the counter and reference electrodes respectively for three electrode system measurements. The utilized electrolytes were 1 M LiCl and 1 M $AlCl_3$ aqueous electrolytes unless otherwise stated. The separation between Al and $LiMn_2O_4$ is maintained at 1cm.

[#] *Corresponding author; email: skdas@tezu.ernet.in; Tel: +91-3712275586; Fax: +91-3712267005*

The crystallographic phase identification was performed by using powder X-ray diffraction (XRD, BRUKER AXS D8 FOCUS; Cu-Kα radiation, $\lambda = 1.5406$ Å) with a scanning rate of 1^{o} min^{-1} in the 2θ range of $10\text{-}70^{o}$ at a generator voltage of 30 KV and current of 30 mA. The morphology was observed by field emission scanning electron microscopy (FESEM, JEOL JSM 7200F) and transmission electron microscopy (TEM, FEI TecnaiG2 20 S-TWIN) at an accelerating voltage of 200 KV. XPS was recorded with Thermo-ScientificESCALAB Xi^{+} spectrometer with a monochromatic Al Kα X-ray source (1486.6 eV). An energy step size of 0.1 eV were used with a dwell time of 50 ms and 10-15 repetitions. For ex-situ XRD, SEM and XPS measurements, the electrodes were harvested after required discharge/charge cycles and washed with deionized water and dried at 110 ^{o}C for 24 hr. For ex-situ XRD, electrodes were prepared with graphite current collector. All the electrochemical experiments were conducted at room temperature (25 ^{o}C).

The electrochemical stability window of the electrolyte was examined using CV experiments, by constructing an Al-Ti cell (breadth 1 cm and length 1.5 cm) in a voltage range of 0.2 V- 2V at a scan rate of 2.5 mVs^{-1}. The aqueous electrolytes were 1 M $AlCl_3$, 0.5 M $Al_2(SO_4)_3$ and 1 M $Al(NO_3)_3$ respectively.

Supplementary figures

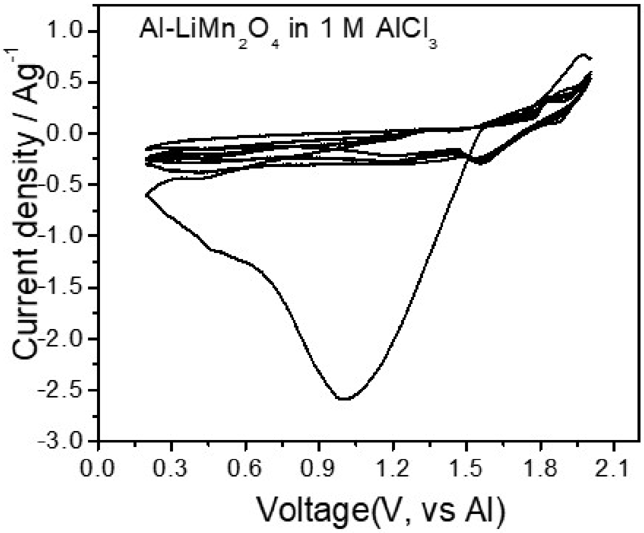

Figure S1. CV curves of LiMn$_2$O$_4$in 1 M AlCl$_3$ aqueous electrolyte at a scan rate of 2.5 mVs^{-1}.

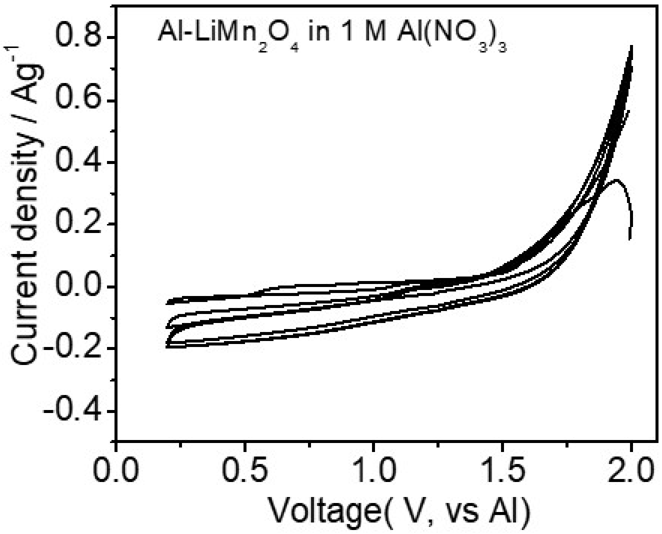

Figure S2: CV curves of LiMn$_2$O$_4$in 1 M Al(NO$_3$)$_3$ aqueous electrolyte at a scan rate of 2.5 mVs^{-1}

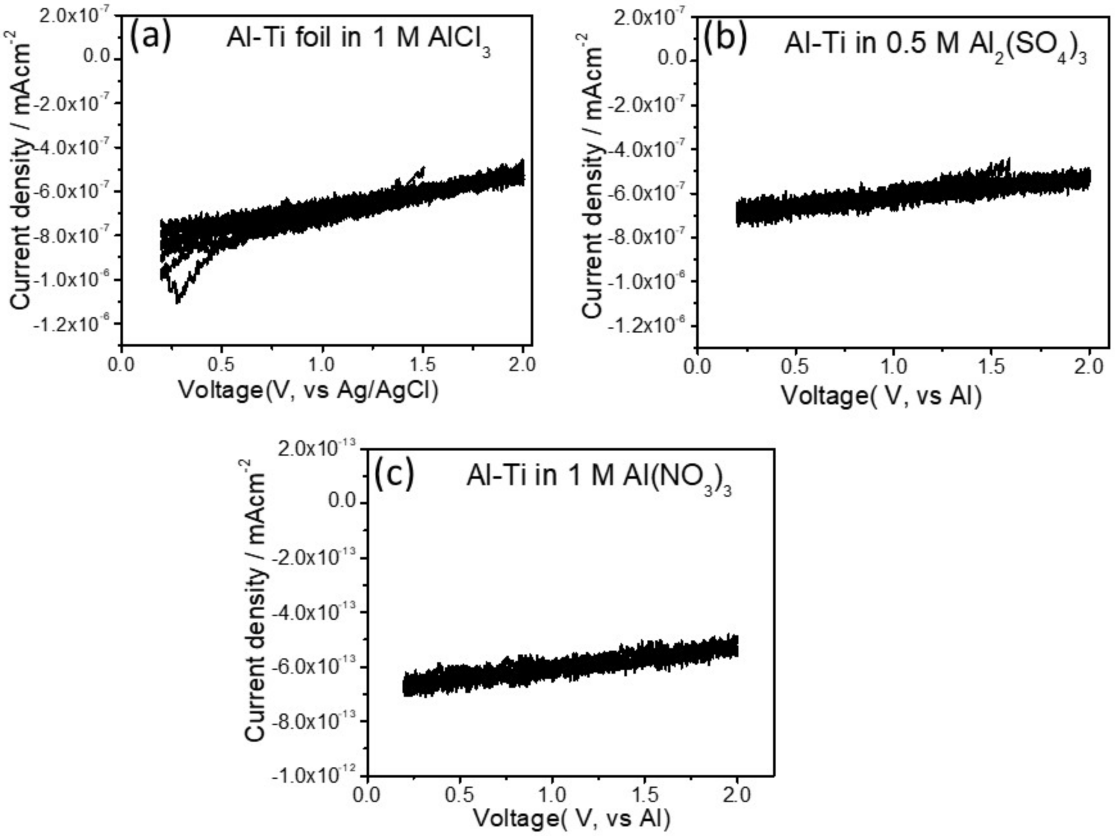

Figure S3: CV curves of Al-Ti cell in (a) 1 M $AlCl_3$, (b) 0.5 M $Al_2(SO_4)_3$, and (c) 1 M $Al(NO_3)_3$ aqueous electrolytes at a scan rate of 2.5mVs^{-1}.

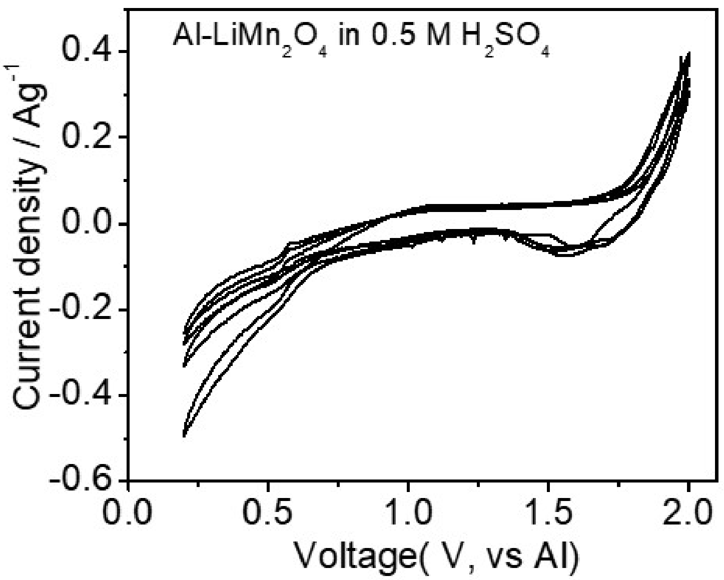

Figure S4: CV curves of $LiMn_2O_4$ in 0.5 M H_2SO_4 aqueous electrolyte at a scan rate of 2.5mVs^{-1}

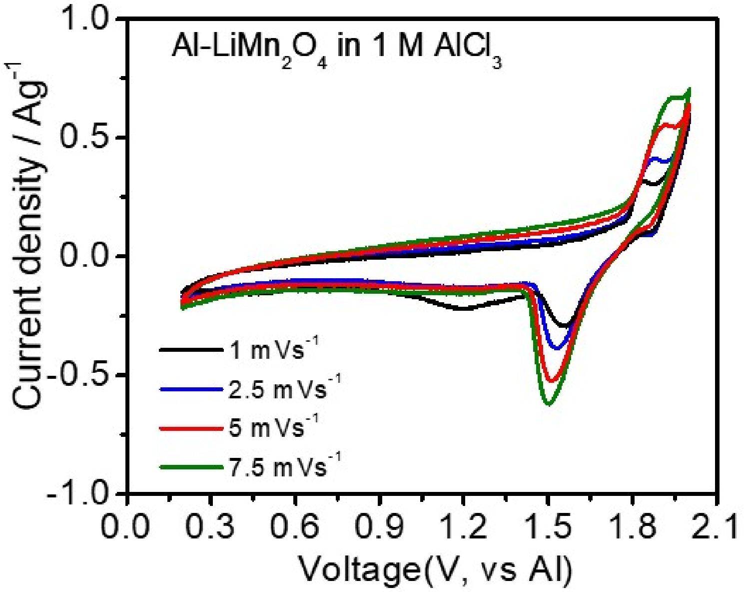

Figure S5: CV curves of $LiMn_2O_4$ in 1 M $AlCl_3$ aqueous electrolyte at different scan rates.

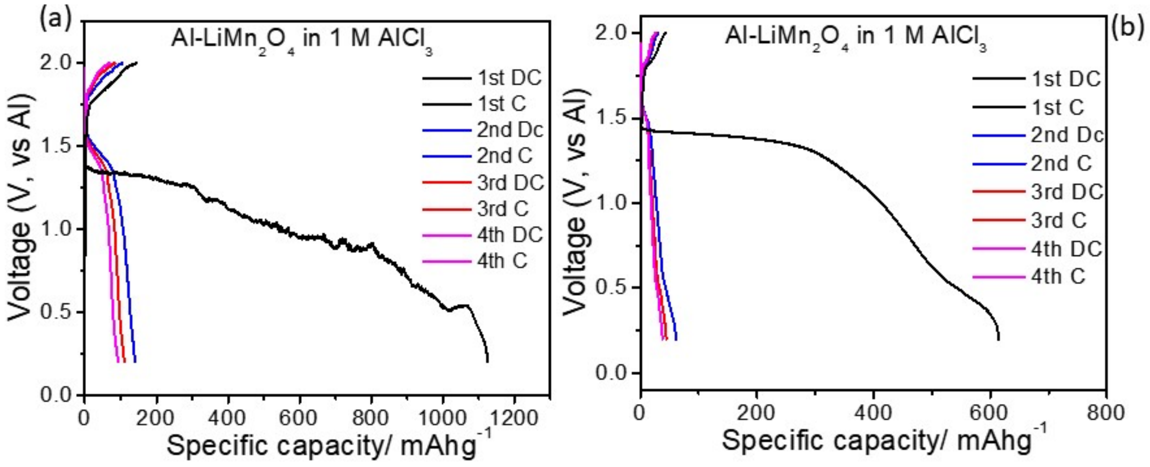

Figure S6: Galvanostatic discharge/charge curves of $LiMn_2O_4$ in 1 M $AlCl_3$at a current rate of (a) 200 $mAg^{-1}$and (b) 600 mAg^{-1}. DC-discharge cycle, C-charge cycle

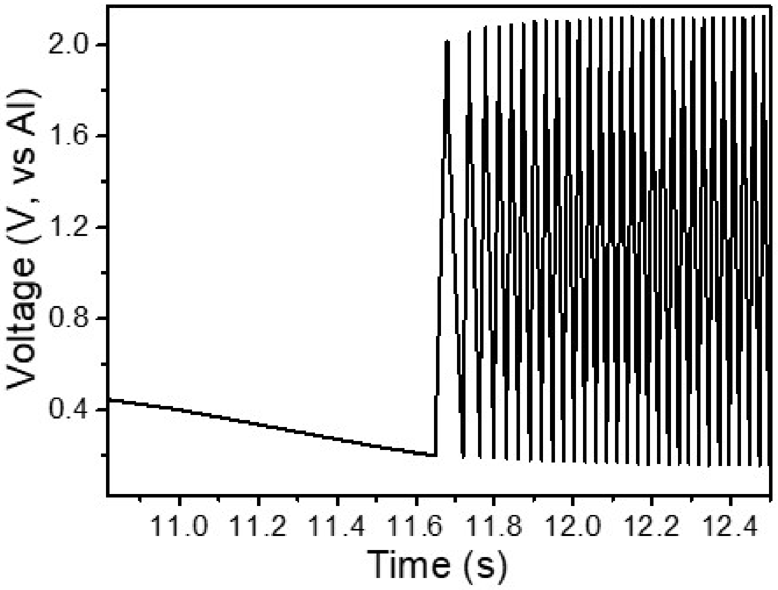

Figure S7: Galvanostatic discharge/charge curves of $LiMn_2O_4$in 0.5M $Al_2(SO_4)_3$ aqueous electrolytes. The current rate is 200mAg^{-1}.

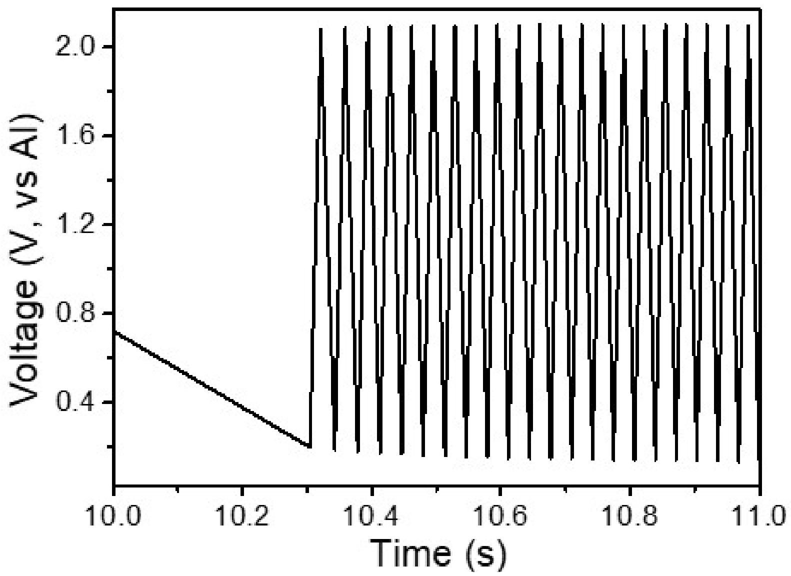

Figure S8: Galvanostatic discharge/charge curves of $LiMn_2O_4$in 1M $Al(NO_3)_3$ aqueous electrolytes. The current rate is 200mAg^{-1}.

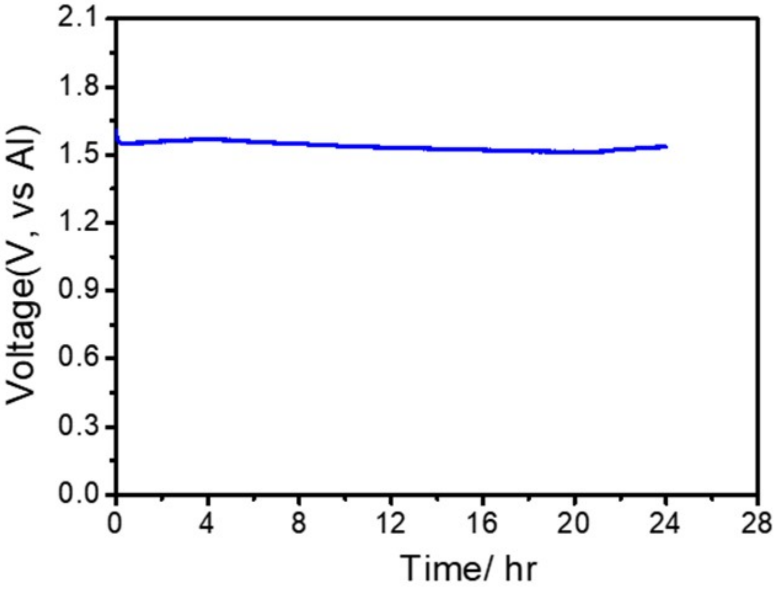

Figure S9: Self-discharge profile of Al-$LiMn_2O_4$ cell in 1 M $AlCl_3$ aqueous electrolyte.

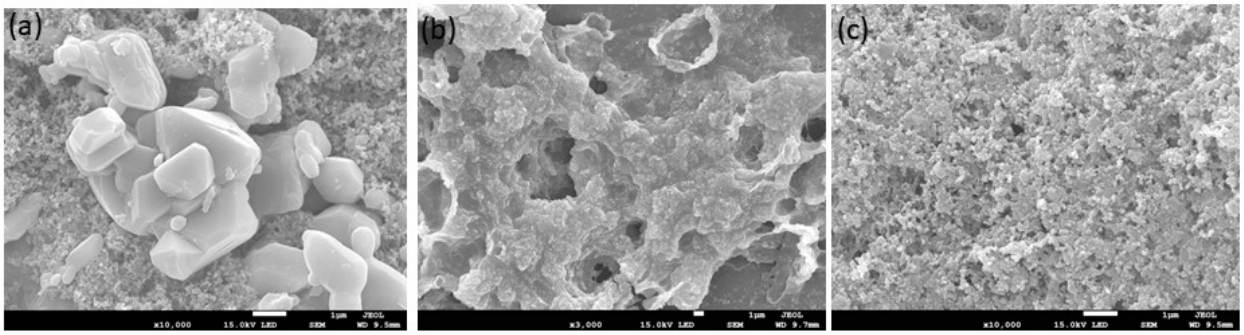

Figure S10: Ex-situ FESEM images of $LiMn_2O_4$ electrode (a) before discharge, (b) after 1st discharge and (c) after 1st charge.

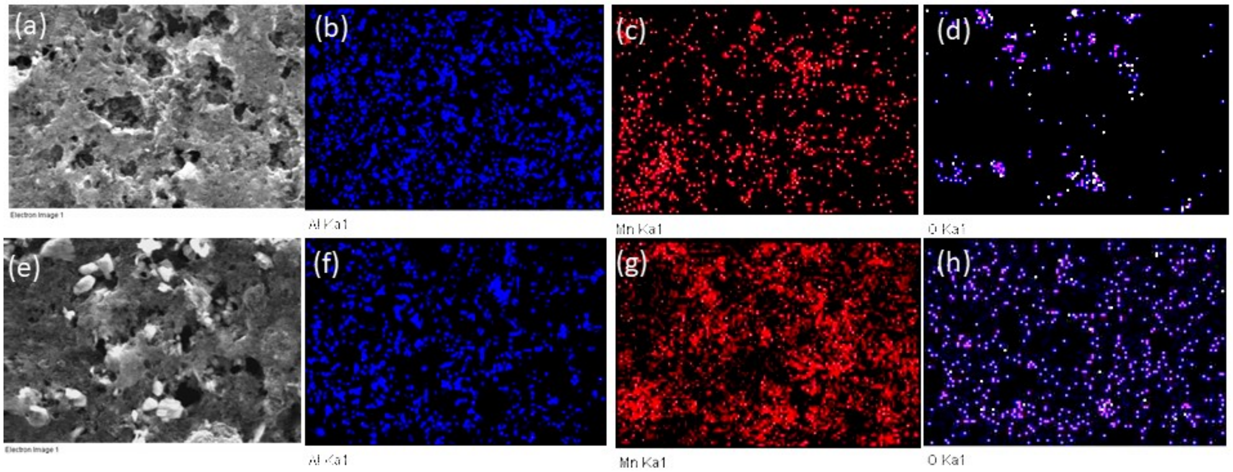

Figure S11: (a) SEM image of scanned area for elemental mapping of 1st discharge state $LiMn_2O_4$ electrode. Elemental mapping images of (b) Al, (c) Mn and (d) O of the 1st discharge state electrode. (e) SEM image of scanned area for elemental mapping of 1st charge state $LiMn_2O_4$ electrode. Elemental mapping images of (f) Al, (g) Mn and (h) O of the 1st charge state electrode.

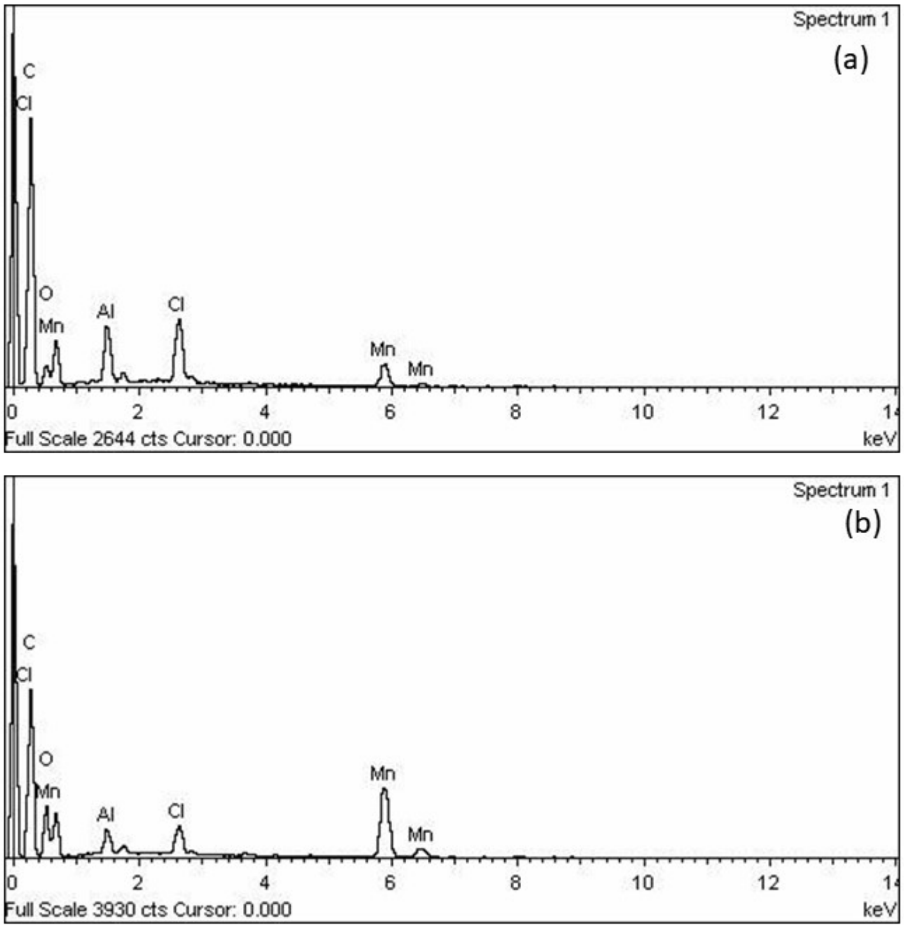

Figure S12: Energy dispersive X-ray (EDX) spectrum of $LiMn_2O_4$ (a) after 1st discharge state electrode and (b) after 1st charge electrode

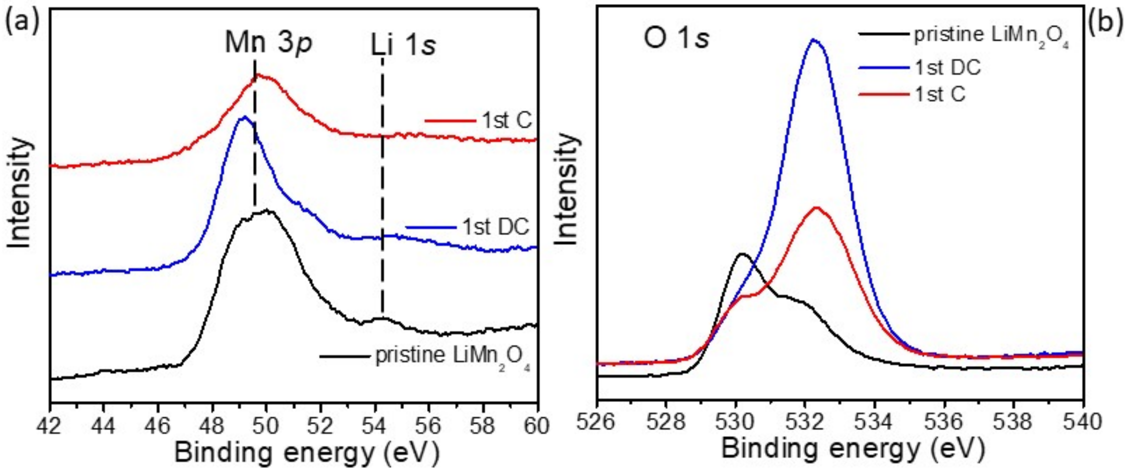

Figure S13: (a) Li 1s and (b) O 1s XPS spectra of $LiMn_2O_4$ electrode before discharge, after 1st discharge and after 1st charge.

Table S1: The electrochemical performances of other cathode materials

Cathode materials	Discharge capacity ($mAhg^{-1}$)[a]	current density (mAg^{-1})	Type of electrolyte	Reference
$LiMn_2O_4$	65	800	Aqueous electrolyte	this work
MnO_2	380	100	Aqueous electrolyte	S1
MnO_2	467	30	Aqueous electrolyte	S2
$FeVO_4$	350	60	Aqueous electrolyte	S3
$Na_3V_2(PO_4)_3$	60-100	60	Aqueous electrolyte	S4
V_2O_5 aerogel	120	60	Aqueous electrolyte	S5
MoO_3	170	2500	Aqueous electrolyte	S6
Graphite	88	500	Aqueous electrolyte	S7
Prussian blue	41	400	Aqueous electrolyte	S8
TiO_2	180	50	Aqueous electrolyte	S9
Graphene-TiO_2	33-50	6250	Aqueous electrolyte	S9

(a) The highest discharge capacity is mentioned

Reference:

S1. Q. Zhao, M. J. Zachman, W. I. A. Sadat, J. Zheng, L. F. Kourkoutis and L. Archer, *Sci. Adv.*, 2018, **4**,8131.

S2. C. Wu, S. Gu, Q. Zhang, Y. Bai, M. Li, Y. Yuan, H. Wang, X. Liu, Y. Yuan, N. Zhu, F. Wu, H. Li, L. Gu and J. Lu, *Nat. Commun.*, 2019, **10**, 1–10.

S3. S. Kumar, R. Satish, V. Verma, H. Ren, P.Kidkhunthod, W. Manalastas Jr. and M. Srinivasan, *J. Power Sources*, 2019, **426**, 151–161.

S4. F. Nacimiento, M. Cabello, R. Alcantara, P.Lavela and J. L. Tirado, *Electrochimica Acta*, 2019, **260**, 798-804.

S5. J. R. González, F. Nacimiento, M. Cabello, R. Alcántara, P. Lavelaa and J. L. Tiradoa, *RSC Adv.*, 2016,**6**, 62157-62164.

S6. H. Lahan and S. K. Das, *J. Power Sources*, 2019, **413**, 134.

S7. S. Nandi and S. K.Das, *ACS Sustain. Chem. Eng*. 2019, **7**, 19839-19847.

S8. S. Liu, G. L. Pan, G. R. Li and X. P. Gao, *J. Mater. Chem. A*, 2015, **3**, 959-962.

S9. M. Kazazi, P. Abdollahi and M. Mirzaei-Moghadam, *State Ionics*, 2017, **300**, 32–37.

S10. H. Lahan, Ratan Boruah, Anil Hazarika and S. K. Das, *J. Phys. Chem. C*, 2017, **121**, 47, 26241–26249